International Journal of Industrial Engineering Computations 12 (2021) 401–414

Contents lists available at GrowingScience

International Journal of Industrial Engineering Computations

homepage: www.GrowingScience.com/ijiec

A homogenously weighted moving average scheme for observations under the effect of serial dependence and measurement inaccuracy

Maonatlala Thanwane[a], Sandile C. Shongwe[b*], Muhammad Aslam[c], Jean-Claude Malela-Majika[d] and Mohammed Albassam[c]

[a]*Department of Statistics, College of Science, Engineering and Technology, University of South Africa, South Africa*
[b]*Department of Mathematical Statistics and Actuarial Science, Faculty of Natural and Agricultural Sciences, University of the Free State; Bloemfontein 9301, South Africa*
[c]*Department of Statistics, Faculty of Science, King Abdulaziz University, Jeddah 21551, Saudi Arabia*
[d]*Department of Statistics, Faculty of Natural and Agricultural Sciences, University of Pretoria, Hatfield 0002, South Africa*

C H R O N I C L E

Article history:
Received December 28 2020
Received in Revised Format
April 31 2021
Accepted May 11 2021
Available online
May, 11 2021

Keywords:
Autocorrelation
Control chart
Homogeneously weighted moving average (HWMA)
Measurement errors
Mixed samples strategy
Multiple measurements
Skipping sampling strategy

A B S T R A C T

The combined effect of serial dependency and measurement errors is known to negatively affect the statistical efficiency of any monitoring scheme. However, for the recently proposed homogenously weighted moving average (HWMA) scheme, the research that exists concerns independent and identically distributed observations and measurement errors only. Thus, in this paper, the HWMA scheme for monitoring the process mean under the effect of within-sample serial dependence with measurement errors is proposed for both constant and linearly increasing measurement system variance. Monte Carlo simulation is used to evaluate the run-length distribution of the proposed HWMA scheme. A mixed-*s&m* sampling strategy is incorporated to the HWMA scheme to reduce the negative effect of serial dependence and measurement errors and its performance is compared to the existing Shewhart scheme. An example is given to illustrate how to implement the proposed HWMA scheme for use in real-life applications.

1. Introduction

Monitoring schemes are efficient tools in statistical process monitoring (SPM) as they aim at efficiently monitoring streaming processes and detecting changes in process performance, as early as possible, so that corrective measures can be taken to ensure a minimal loss due to a downfall in the quality of whatever process that is monitored. More importantly, the main goal of a monitoring scheme is to provide a way to distinguish between two sources of variability, i.e. chance and assignable causes of variability. When a process runs only in the presence of chance causes of variation, it is said to be in a state of in-control (IC). However, when it runs in the presence of assignable causes (this can be as a result of additional variations that are caused by machinery, human and/or material error), the process is said to be out-of-control (OOC). Any efficient monitoring scheme needs to respond to changes in the quality characteristic of interest as early as possible to aid in eliminating or reducing unwanted waste, see Montgomery (2013). It has been proven that monitoring schemes like Shewhart-type schemes are more efficient in detecting large shifts; while memory-type schemes like the exponentially weighted moving average (EWMA), cumulative sum (CUSUM) and the generally weighted moving average (GWMA) tend to be more efficient in detecting small shifts. More recently, Abbas (2018) proposed a new memory-type scheme called the homogeneously weighted moving average (HWMA) $\bar{X}$ control chart to monitoring the mean of independent and identically distributed (i.i.d.) observations.

* Corresponding author Tel.: +27648482001
E-mail: shongwesc@ufs.ac.za (S. C. Shongwe)

2021 Growing Science Ltd.
doi: 10.5267/j.ijiec.2021.5.003

Other HWMA schemes are discussed in Nawaz and Han (2020), Adegoke et al. (2020a, b), Abbas et al. (2020), Dawod et al. (2020), Raza et al. (2020). Note that the HWMA scheme allocates a specific weight to the current sample and the remaining weight is distributed equally (or homogeneously) among all the previous samples. Other extended HWMA schemes for i.i.d. observations have been studied in Adeoti and Koleoso (2020), Abid et al. (2020a, b), Malela-Majika et al. (2021) and Alevizakos et al. (2021). More recently, Thanwane et al. (2020) studied the effect of measurement errors on the performance of the HWMA scheme and here, the focus is on the combined effect of measurement errors and serial dependency (also known as autocorrelation). For separate literature reviews on autocorrelated processes and processes with measurement errors in a SPM context, see Prajapati and Singh (2012) and Maleki et al. (2017), respectively.

In this paper, the well-known first-order autoregressive model (i.e. AR(1)) is considered as a starting point (other models will be discussed in upcoming articles). The AR(1) model with positive autocorrelation is the most commonly used time series model in SPM applications due to its simplicity as compared to other stationary time series models. For other discussions on AR(1) model in a univariate or multivariate SPM context, see for example: Ahmad et al. (2019), Dargopatil and Ghute (2019), Oh and Weiβ (2020). Note that if the process remains in equilibrium around the constant mean then the autocorrelated process is IC; however, when there is any statistically significant difference from the constant mean, it implies that the autocorrelated process is OOC. To reduce the negative effect of autocorrelation, there are some sampling strategies that exist that are used in effectively improving the performance of any monitoring scheme, to count a few: the *s*-skip (by Costa and Castagliola, 2011), mixed samples (by Franco et al., 2014) and mixed-*s*-skip (by Shongwe et al., 2021). In the latter, *s* denotes the number of observations that must be skipped before sampling to form a rational subgroup. The review paper by Maleki et al. (2017) stated that, even with highly sophisticated advanced measuring instruments, an exact measurement is a rare phenomenon; hence, measurement errors tend to exist in any manufacturing and service environment. To account for measurement errors, the additive model (or linear covariate error) model with a constant and linearly increasing variance are used, see for instance Linna and Woodall (2001), Maravelakis et al. (2004) and Maravelakis (2012). The most used remedial strategy to reduce the negative effect of measurement errors is the *m*-measurements approach by Linna and Woodall (2001), which entails measuring each observation m times. Some recent contributions to monitoring schemes under the effect of measurement error are provided in Nguyen et al. (2020), Zaidi et al. (2020), Asif et al. (2020) and Arif et al. (2020). Yang and Yang (2005), Xiaohong and Zhaojun (2009), Costa and Castagliola (2011), Shongwe et al. (2020, 2021), Shongwe and Malela-Majika (2020) considered some monitoring schemes where the process mean is assumed to be under the combined effect of autocorrelation and measurement errors. It has been generally concluded that the combined effect of autocorrelation and measurement errors has a higher negative effect on the performance of any monitoring schemes than the latter two factors, individually. Therefore, the most important contribution of this paper is to propose a *dedicated* HWMA $\bar{X}$ scheme, where autocorrelated observations with measurement errors are likely to occur.

The rest of this paper is organised as follows: In Section 2, the main properties of the HWMA scheme for monitoring i.i.d observations is discussed. Section 3 introduces the HWMA scheme for monitoring the process mean under the combined effect of autocorrelation and measurement errors. The empirical performance of the proposed HWMA scheme is given in Section 4. An illustrative example showing how to implement the proposed HWMA scheme is provided in Section 5. Finally, some concluding remarks are presented in Section 6.

2. Design of the basic HWMA scheme for i.i.d. observations

Let the sequence of observations $X_{ti}\{t = 1, 2, \ldots, \text{and } i = 1, 2, \ldots, n\}$ be a set of samples of i.i.d. normal random variables, i.e. $X_{ti} \sim N(\mu_0 + \delta\sigma_0, \sigma_0)$, where μ_0 is the IC mean value, σ_0 is the IC standard deviation and δ is the magnitude of the shift in standard deviation units. When $\delta = 0$, it implies that $X_{ti} \sim N(\mu_0, \sigma_0)$ and hence, the process is considered to be IC. However, when $\delta \neq 0$, the process is OOC. Let $\bar{X}_t = \sum_{i=1}^{n} X_{ti}/n$ be the sample mean of the t^{th} subgroup; then the plotting statistic of the HWMA $\bar{X}$ scheme (denoted as H_t) is defined as

$$H_t = \lambda\bar{X}_t + (1-\lambda)\,\bar{\bar{X}}_{t-1} = \lambda\bar{X}_t + (1-\lambda)\left(\frac{1}{t-1}\sum_{v=1}^{t-1}\bar{X}_v\right). \tag{1}$$

Note that λ is the smoothing constant (where $0 < \lambda \leq 1$) and $\bar{\bar{X}}_{t-1}$ is the mean of the previous $t-1$ subgroup sample means, with $\bar{\bar{X}}_0$ (i.e. when t=1) set to be equal to the target mean μ_0; see Abbas (2018). It is apparent that the charting statistic H_t assigns a weight λ to the current sample and a weight $(1-\lambda)$ is homogeneously (or equally) distributed to the previous $t-1$ samples. Abbas (2018) showed that the mean and standard deviation of H_t are given by

$$E(H_t) = \mu_0 \tag{2}$$

and

$$\sigma_{H_t} = \begin{cases} \sqrt{\lambda^2\dfrac{\sigma_0^2}{n}}, & t = 1 \\ \sqrt{\lambda^2\dfrac{\sigma_0^2}{n} + (1-\lambda)^2\dfrac{\sigma_0^2}{n(t-1)}}, & t > 1 \end{cases} \tag{3}$$

respectively. Note that the average run-length (*ARL*), defined as the mean of the run-length distribution or the average number of rational subgroups plotted on a control chart before it gives a signal for the first time, is the most used run-length metric in SPM literature. This metric reveals the degree of the sensitivity of a monitoring scheme towards specific shifts. Thereafter, Abbas (2018) showed that the time-varying lower and upper control limits (i.e. LCL_t and UCL_t) of the HWMA $\bar{X}$ monitoring scheme are defined by

$$LCL_t = \begin{cases} \mu_0 - L\sqrt{\lambda^2 \frac{\sigma_0^2}{n}}, & t = 1 \\ \mu_0 - L\sqrt{\lambda^2 \frac{\sigma_0^2}{n} + (1-\lambda)^2 \frac{\sigma_0^2}{n(t-1)}}, & t > 1 \end{cases} \tag{4a}$$

and

$$UCL_t = \begin{cases} \mu_0 + L\sqrt{\lambda^2 \frac{\sigma_0^2}{n}}, & t = 1 \\ \mu_0 + L\sqrt{\lambda^2 \frac{\sigma_0^2}{n} + (1-\lambda)^2 \frac{\sigma_0^2}{n(t-1)}}, & t > 1 \end{cases} \tag{4b}$$

respectively; where $L > 0$ is the control limits constant that is set in order to have an IC ARL approximately equal to some pre-specified nominal IC ARL (i.e. ARL_0). Thus, the HWMA $\bar{X}$ scheme gives a signal if $H_t \geq UCL_t$ or $H_t \leq LCL_t$. In case the process has been running for a long time (i.e. $t \to \infty$), the term $\frac{\sigma_0^2}{n(t-1)} \to 0$. Therefore, the control limits in (4a) and (4b) reduce to the following asymptotic ones:

$$UCL/LCL = \mu_0 \pm L\sqrt{\lambda^2 \frac{\sigma_0^2}{n}}. \tag{5}$$

3. HWMA scheme for monitoring autocorrelated observations with measurement errors

3.1 AR(1) process incorporated in the covariate error model

Let the sequence of observations $X_{ti}^{\#}$ $\{t = 1, 2,\ldots,$ and $i = 1, 2, \ldots, n\}$ be a set of samples of autocorrelated $N(\mu_0 + \delta\sigma_0, \sigma_0)$ distribution that fits a stationary AR(1) model, given by

$$X_{t,i}^{\#} - \mu_0 = \phi\left(X_{t-1,i}^{\#} - \mu_0\right) + \varepsilon_t, t \geq 1, \quad i = 1, 2, \ldots, n; \tag{6}$$

where ϕ is the level of serial dependence (or autocorrelation) assumed to satisfy $0 < \phi < 1$ and ε_t are i.i.d. $N(0,\sigma_\varepsilon)$ random variables, with $\sigma_0 = \frac{\sigma_\varepsilon}{\sqrt{1-\phi^2}}$ and, without loss of generality, it is assumed that $\sigma_\varepsilon = 1$. Let $\bar{X}_t^{\#}$ be the sample mean of the t^{th} subgroup and while it is assumed that there is dependence within the computation of $\bar{X}_t^{\#}$; however, between any $\bar{X}_t^{\#}$ and $\bar{X}_w^{\#}$ $(t \neq w)$ there is independence which means no cross-correlation, see Alwan and Radson (1992). Assume that the true value of $X_{t,i}^{\#}$ defined in (6) is only observed through a value $\{X_{t,i,j}^{*}$: t = 1,2,…; i = 1,…, n; j = 1,…, $m\}$ described by the expression $X_{t,i,j}^{*} = A + BX_{t,i}^{\#} + \varepsilon_{t,i,j}$, where A and B are two constants depending on the measurement system location error. It is worth mentioning that Costa and Castagliola (2011) and Shongwe et al. (2021) considered the case where $A = 0$ and $B = 1$ only. Note that m denotes the number of measurements taken in each sampled subgroup unit and $\varepsilon_{i,j,k} \sim N(0, \sigma_M^2)$ is a random error due to the measurement error that is distributed independently of $X_{t,i}^{\#}$; where σ_M^2 is the variance of the measurement system. Based on the discussion in Linna and Woodall (2001), Maravelakis et al (2004) and Maravelakis (2012), it is apparent that $X_{t,i,j}^{*} \sim N(A + B\mu_0, B^2\sigma_0^2 + \sigma_M^2)$. Assuming that n observations from the sequence $X_{t,i,j}^{*}$ at each sampling point have been collected, then using the mixed-s-skip with m-measurements (denoted as mixed-s&m) strategy, the process mean is calculated as follows

$$\bar{X}_t^{*} = A + B\frac{1}{n}\left(\sum_{i=1}^{n_{t-1}} X_{t-1,(s+1)i}^{\#} + \sum_{i=1}^{n_t} X_{t,(s+1)i-s}^{\#}\right) + \frac{1}{nm}\sum_{i=1}^{n}\sum_{j=1}^{m} \varepsilon_{t,(s+1)i-s,j}\,; \tag{7}$$

however, for the no remedy strategy (i.e. s=0 and m=1), it is calculated by

$$\bar{X}_t^{*} = A + B\frac{1}{n}\sum_{i=1}^{n} X_{t,i}^{\#} + \frac{1}{nm}\sum_{i=1}^{n}\sum_{j=1}^{1} \varepsilon_{t,i,j}\,; \tag{8}$$

see for instance Costa and Castagliola (2011) and Shongwe et al. (2021). Since between any $\bar{X}_t^{\#}$ and $\bar{X}_w^{\#}$ $(t \neq w)$ there is independence, it follows that

$$Cov(\bar{X}_t^{*}, \bar{X}_w^{*}) = 0, \text{ for any } t \neq w. \tag{9}$$

In the case of constant measurement system variance, let $\gamma = \frac{\sigma_M}{\sigma_0}$ represents the standardized ratio of the measurement system variability to the process variability. Then, from Costa and Castagliola (2011), it follows that when the 'no remedy' strategy is implemented, the expected value and variance of $\bar{X}_t^*$ are respectively given by

$$E(\bar{X}_t^*) = A + B\mu_0, \tag{10}$$

and

$$Var(\bar{X}_t^*) = \frac{\sigma_0^2}{n}\left(\left(1 + 2\left(\frac{\phi^{n+1} - n\phi^2 + (n-1)\phi}{n(\phi-1)^2}\right)\right) + (B^2 + \gamma^2) - 1\right). \tag{11a}$$

In some situations, the measurement error σ_M^2 should no longer be considered as being a constant but it should be considered as an increasing function of the mean of the variable $X_{t,i}^{\#}$, i.e. $\sigma_M^2 = C + D\mu_0$ and thus, $X_{t,i,j}^* \sim N(A + B\mu_0, B^2\sigma_0^2 + C + D\mu_0)$, where C and D are two constants. It is worth mentioning that Costa and Castagliola (2011) and Shongwe et al. (2021) did not consider the linearly increasing variance scenario. Following similar steps as done for (10) and (11), it follows that for linearly increasing measurement system variance, the expected value of $\bar{X}_t^*$ for the 'no remedy' strategy is given by (10). However, the variance of $\bar{X}_t^*$ is given by

$$Var(\bar{X}_t^*) = \frac{\sigma_0^2}{n}\left(\left(1 + 2\left(\frac{\phi^{n+1} - n\phi^2 + (n-1)\phi}{n(\phi-1)^2}\right)\right) + \left(B^2 + \frac{C + D\mu_0}{\sigma_0^2}\right) - 1\right). \tag{11b}$$

Note that when the mixed-$s\&m$ strategy is implemented, the expected value of $\bar{X}_t^*$ is the same as that in (10); however, the variance of $\bar{X}_t^*$ is given by

$$Var(\bar{X}_t^*) = \frac{\sigma_0^2}{n}\varphi. \tag{12a}$$

where φ for the constant measurement system variance is given by

$$\begin{aligned}\varphi = &\left(\frac{n_t}{n} + 2\left(\frac{\phi^{(s+1)(n_t+1)} - n_t\phi^{2s+2} + (n_t-1)\phi^{s+1}}{n(\phi^{s+1}-1)^2}\right)\right) \\ &+ \left(\frac{n_{t-1}}{n} + 2\left(\frac{\phi^{(s+1)(n_{t-1}+1)} - n_{t-1}\phi^{2s+2} + (n_{t-1}-1)\phi^{s+1}}{n(\phi^{s+1}-1)^2}\right)\right) + \left(B^2 + \frac{\gamma^2}{m}\right) - 1,\end{aligned} \tag{12b}$$

and for the linearly increasing measurement system variance, it is given by

$$\begin{aligned}\varphi = &\left(\frac{n_t}{n} + 2\left(\frac{\phi^{(s+1)(n_t+1)} - n_t\phi^{2s+2} + (n_t-1)\phi^{s+1}}{n(\phi^{s+1}-1)^2}\right) + \frac{n_{t-1}}{n}\right. \\ &\left. + 2\left(\frac{\phi^{(s+1)(n_{t-1}+1)} - n_{t-1}\phi^{2s+2} + (n_{t-1}-1)\phi^{s+1}}{n(\phi^{s+1}-1)^2}\right)\right) + \left(B^2 + \frac{C + D\mu_0}{m\sigma_0^2}\right) - 1.\end{aligned} \tag{12c}$$

3.2 Properties and operation of the HWMA $\bar{X}^*$ scheme with mixed-$s\&m$ strategy

Based on the discussion in Sections 2 and 3.1, it follows that the plotting statistic of the HWMA $\bar{X}^*$ scheme with mixed-$s\&m$ strategy is defined by

$$H_t^* = \lambda\bar{X}_t^* + (1-\lambda)\,\bar{\bar{X}}_{t-1}^* = \lambda\bar{X}_t^* + (1-\lambda)\left(\frac{1}{t-1}\sum_{v=1}^{t-1}\bar{X}_v^*\right), \tag{13}$$

where $\bar{\bar{X}}_{t-1}^*$ is the mean of the previous $t-1$ sample means, with $\bar{\bar{X}}_0^*$ (i.e. $t = 1$) set to be equal to the target mean in (10), that is,

$$\bar{\bar{X}}_0^* = A + B\mu_0. \tag{14}$$

Using the Eq. (10), it follows that the expected value of H_t^* is given by

$$E(H_t^*) = \lambda E(\bar{X}_t^*) + \frac{1-\lambda}{t-1}\sum_{v=1}^{t-1}E(\bar{X}_v^*) = \lambda(A + B\mu_0) + \frac{1-\lambda}{t-1}\sum_{v=1}^{t-1}(A + B\mu_0) = A + B\mu_0. \tag{15}$$

To calculate the variance of Eq. (13), the following need to be determined

$$Var(H_t^*) = \lambda^2 Var(\bar{X}_t^*) + (1-\lambda)^2 Var\left(\bar{\bar{X}}_{t-1}^*\right) + 2\sum\sum Cov\left(\bar{X}_t^*, \bar{\bar{X}}_{t-1}^*\right). \tag{16}$$

Firstly, the expression of the $Var(\bar{X}_t^*)$ are provided in (12a) to (12c) for the mixed-$s\&m$ strategy in the case of constant and linearly increasing measurement system variance. Secondly, the expressions of $Var\left(\bar{\bar{X}}_{t-1}^*\right)$ is determined in two parts, i.e. for $t = 1$ and $t > 1$. That is, for $t = 1$, using Eq. (14), it follows that

$$Var\left(\bar{\bar{X}}_0^*\right) = Var(A + B\mu_0) = 0. \tag{17a}$$

However, for $t > 1$, using (9) and (12a), it follows that

$$
\begin{aligned}
Var\left(\bar{\bar{X}}^*_{t-1}\right) &= Var\left(\frac{1}{t-1}\sum_{v=1}^{t-1}\bar{X}^*_v\right) \\
&= \left(\frac{1}{t-1}\right)^2\sum_{v=1}^{t-1}Var(\bar{X}^*_i) + 2\sum_{v<l}\sum Cov(\bar{X}^*_v,\bar{X}^*_l) \\
&= \left(\frac{1}{t-1}\right)^2\sum_{v=1}^{t-1}Var(\bar{X}^*_v) \\
&= \left(\frac{1}{t-1}\right)^2\sum_{v=1}^{t-1}\frac{\sigma_0^2}{n}\varphi \\
&= \left(\frac{1}{t-1}\right)\frac{\sigma_0^2}{n}\varphi.
\end{aligned}
\tag{17b}
$$

Thirdly, since $\bar{\bar{X}}^*_{t-1} = \frac{1}{t-1}(\bar{X}^*_1 + \bar{X}^*_2 + \cdots + \bar{X}^*_{t-1})$, then from (9), it follows that

$$
2\sum\sum Cov\left(\bar{X}^*_t, \bar{\bar{X}}^*_{t-1}\right) = 2\sum\sum Cov\left(\bar{X}^*_t, \frac{1}{t-1}(\bar{X}^*_1 + \bar{X}^*_2 + \cdots + \bar{X}^*_{t-1})\right) = 0. \tag{17c}
$$

Thus, substituting Eq. (17a) to Eq. (17c) in Eq. (16), when t =1 and t >1, it follows that

$$
Var(H^*_t) = \begin{cases} \lambda^2\dfrac{\sigma_0^2}{n}\varphi, & \text{when } t = 1 \\ \lambda^2\dfrac{\sigma_0^2}{n}\varphi + (1-\lambda)^2\left(\dfrac{1}{t-1}\right)\dfrac{\sigma_0^2}{n}\varphi, & \text{when } t > 1. \end{cases} \tag{18}
$$

Therefore, using Eq. (15) and Eq. (18), it follows that the time-varying lower and upper control limits (i.e. LCL_t and UCL_t) of the HWMA $\bar{X}^*$ scheme with mixed-$s\&m$ strategy are defined by

$$
LCL_t = \begin{cases} (A + B\mu_0) - L^*\sqrt{\lambda^2\dfrac{\sigma_0^2}{n}\varphi}, & \text{when } t = 1 \\ (A + B\mu_0) - L^*\sqrt{\left(\lambda^2\dfrac{\sigma_0^2}{n} + (1-\lambda)^2\dfrac{\sigma_0^2}{n(t-1)}\right)\varphi}, & \text{when } t > 1 \end{cases} \tag{19a}
$$

and

$$
UCL_t = \begin{cases} (A + B\mu_0) + L^*\sqrt{\lambda^2\dfrac{\sigma_0^2}{n}\varphi}, & \text{when } t = 1 \\ (A + B\mu_0) + L^*\sqrt{\left(\lambda^2\dfrac{\sigma_0^2}{n} + (1-\lambda)^2\dfrac{\sigma_0^2}{n(t-1)}\right)\varphi}, & \text{when } t > 1 \end{cases} \tag{19b}
$$

respectively; where $L^* > 0$ is the control limits coefficient that is set to have an IC ARL approximately equal to some pre-specified ARL_0, and φ is as given in (12b) and (12c) for the constant and linearly increasing measurement system variance. Thus, the HWMA $\bar{X}^*$ scheme gives a signal if $H^*_t \geq UCL_t$ or $H^*_t \leq LCL_t$. When the process has been running for a long time, $\frac{\sigma_0^2}{n(t-1)} \to 0$ and thus, Eq. (19a) and EQ. (19b) reduce to the following asymptotic ones:

$$
UCL/LCL = \mu_0 \pm L^*\sqrt{\lambda^2\frac{\sigma_0^2}{n}\varphi}. \tag{20}
$$

Consequently, the operational procedure of the HWMA $\bar{X}^*$ scheme using the mixed-$s\&m$ strategy is summarized in Fig. 1.

4. Performance of the HWMA $\bar{X}^*$ scheme

4.1 Run-length characteristics

To compute the run-length properties (i.e. the *ARL* and the standard deviation of the run-length (*SDRL*)), in this paper, the Monte Carlo simulations approach using SAS v9.4 are used. Note that in addition to the latter, the expected *ARL* (*EARL*) metric is also used to investigate the performance over a range of shifts. The *EARL* is mathematically defined by

$$
EARL_{(\delta_{\min},\delta_{\max}]} = \frac{1}{\Delta}\sum_{\delta=\delta_{min}}^{\delta_{max}} ARL(\delta), \tag{21}
$$

where $\delta_{\min}$ and $\delta_{\max}$ are the lower and upper bound of the shift (δ) parameter, respectively, $ARL(\delta)$ is the *ARL* value for a specific shift δ and Δ represents the number of increments between $\delta_{\min}$ and $\delta_{\max}$. Thus, the $EARL$ values denoted by

$EARL_{(0,1]}$, $EARL_{(0,2]}$, $EARL_{(1,3]}$ and $EARL_{(0,3]}$ are used to investigate the performance of the HWMA $\bar{X}^{\#}$ scheme for small $(0 < \delta \leq 1)$, small-to-moderate $(0 < \delta \leq 2)$, moderate-to-large $(1 < \delta \leq 3)$ and small-to-large $(0 < \delta \leq 3)$ shifts, respectively. To investigate to what extent using a certain sampling strategies when $\phi > 0$ and $\sigma_M^2 > 0$ has deteriorated the HWMA $\bar{X}^*$ scheme's performance as compared to the i.i.d. case (i.e. ϕ=0 and σ_M^2=0), the percentage difference (%Diff) is defined as a percentage difference of *EARL* at some specified value of ϕ and γ (or ϕ, C and D) from the corresponding i.i.d. case, i.e.

$$\%\text{Diff}_{(\delta_{\min},\delta_{\max}]} = \frac{EARL^{*}_{(\delta_{\min},\delta_{\max}]} - EARL^{\text{i.i.d.}}_{(\delta_{\min},\delta_{\max}]}}{EARL^{\text{i.i.d.}}_{(\delta_{\min},\delta_{\max}]}}, \tag{22}$$

where $EARL^{*}_{[\delta_{\min},\delta_{\max}]}$ denotes the *EARL* of the HWMA $\bar{X}^*$ scheme for some specified $\phi > 0$, whereas $EARL^{\text{i.i.d.}}_{[\delta_{\min},\delta_{\max}]}$ denotes the *EARL* of the HWMA $\bar{X}$ scheme when ϕ=0 and σ_M^2=0. Similarly, the expected *SDRL* is defined as

$$ESDRL_{(\delta_{\min},\delta_{\max}]} = \frac{1}{\Delta}\sum_{\delta=\delta_{min}}^{\delta_{max}} SDRL(\delta), \tag{23}$$

and the %Diff of the *ESDRL* can be defined as in Eq. (22) using Eq. (23).

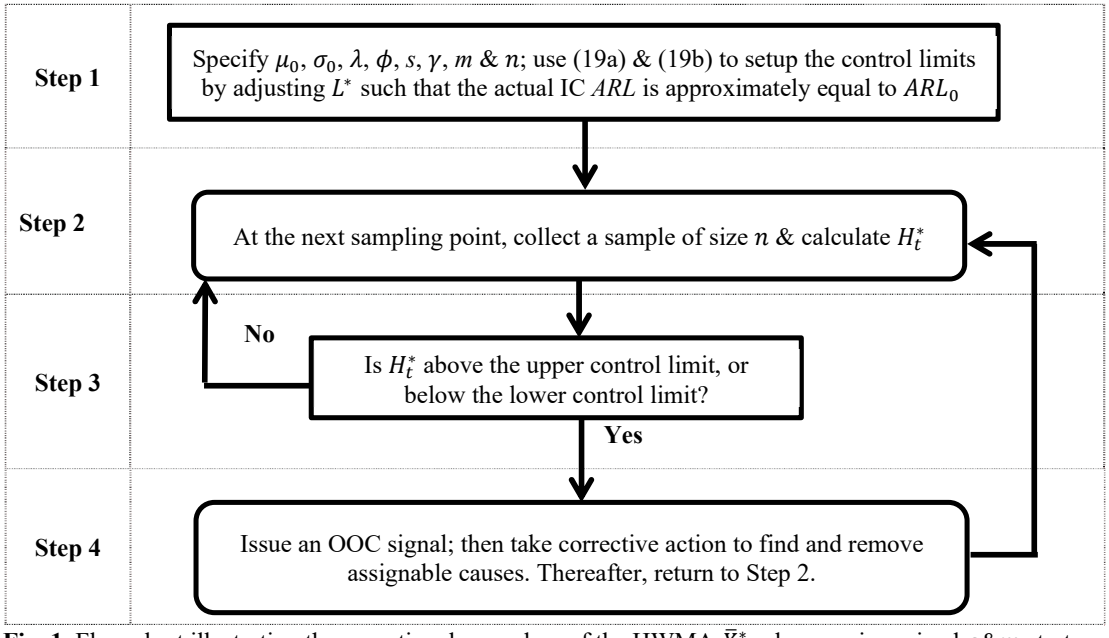

Fig. 1. Flow chart illustrating the operational procedure of the HWMA $\bar{X}^*$ scheme using mixed-s&m strategy

4.2 Sensitivity of the HWMA $\bar{X}^*$ scheme with constant variance

When ϕ and γ are increased, it is observed from Table 1 that the OOC *ARL*s and *SDRL*s of the HWMA $\bar{X}^*$ scheme also increase. Stated differently, for an autocorrelated process with a constant σ_M^2, the performance of the HWMA $\bar{X}^*$ scheme deteriorates as the level of autocorrelation and measurement error increase. For instance, when δ=0.5, the OOC *ARL*s are equal to 7.8, 10.3, 16.3 and 29.0 for both (ϕ,γ) equal to (0,0), (0.2,0.2), (0.5,0.5) and (0.9,0.9), respectively. Similarly, the $EARL_{(0,2]}$ and $ESDRL_{(0,2]}$ increases as both ϕ and γ increase because $\%\text{Diff}_{(0,2]}$ becomes significantly higher as compared to the corresponding i.i.d. values. For instance, the $EARL_{(0,2]}$ of the HWMA $\bar{X}^*$ scheme when (ϕ,γ)=(0.9,0.9) is 206.3% different from the i.i.d. one. Note that similar patterns are observed for other values of the smoothing parameter. Moreover, for a specific value of s and m, the HWMA $\bar{X}^*$ scheme (for the mixed-s&m strategy) has a similar pattern when both ϕ and γ are increased.

When designing the HWMA $\bar{X}^*$ scheme, a user needs to specify a desired λ and then calculate the corresponding L^* such that Step 1 in Figure 1 is satisfied. In Table 2, the effect of λ on the performance of the HWMA $\bar{X}^*$ scheme is illustrated. Except for a few cases when $\delta > 1$, it is observed that as λ increases, the OOC *ARL* and *SDRL* values also increase indicating that the HWMA $\bar{X}^*$ scheme deteriorates in performance. Overall, as λ increases, so do the *EARL* and *ESDRL* values, indicating that, in general, there is a deterioration performance over the majority of shifts. Note that as λ increases, the design parameter L^* increases as well. Stated differently, the control limits of the HWMA $\bar{X}^*$ scheme get wider as λ increases which explains the deterioration of the performance.

Table 1
The *ARL* and *SDRL* profiles of the HWMA $\bar{X}^*$ scheme (for the no remedy strategy) when λ=0.1, n=5, B=1 and ARL_0=500 where $(\phi,\gamma) \in$ {(0.2, 0.2), (0.5,0.5), (0.9,0.9)}

		ARL				*SDRL*			
	(ϕ,γ)	i.i.d.	(0.2,0.2)	(0.5,0.5)	(0.9,0.9)	i.i.d.	(0.2,0.2)	(0.5,0.5)	(0.9,0.9)
	0.0	500.1	502.8	501.0	499.2	407.8	409.6	407.2	409.9
	0.1	95.4	120.4	171.1	252.5	67.5	88.4	133.2	204.6
	0.2	34.0	44.4	67.8	111.7	21.3	29.0	46.0	80.7
	0.3	18.0	23.6	37.0	63.9	10.8	14.6	23.6	43.7
	0.4	11.1	14.8	23.4	40.8	6.3	8.7	14.3	26.5
	0.5	7.8	10.3	16.3	29.0	4.2	5.8	9.5	17.9
	0.6	5.9	7.7	12.0	21.5	3.0	4.2	6.9	13.0
	0.7	4.6	6.1	9.5	16.9	2.3	3.1	5.2	10.0
	0.8	3.9	5.0	7.6	13.5	1.8	2.4	4.1	7.8
δ	0.9	3.3	4.2	6.3	11.1	1.5	2.0	3.3	6.3
	1.0	2.9	3.6	5.4	9.5	1.4	1.7	2.7	5.2
	1.1	2.5	3.2	4.7	8.1	1.2	1.4	2.2	4.4
	1.2	2.2	2.8	4.1	7.1	1.1	1.3	1.9	3.7
	1.3	2.0	2.5	3.7	6.3	1.1	1.2	1.7	3.2
	1.4	1.8	2.3	3.4	5.6	1.0	1.1	1.5	2.8
	1.5	1.6	2.1	3.1	5.0	0.9	1.1	1.4	2.5
	1.6	1.4	1.9	2.8	4.5	0.8	1.0	1.3	2.2
	1.7	1.3	1.7	2.6	4.2	0.7	0.9	1.2	2.0
	1.8	1.2	1.6	2.4	3.9	0.5	0.9	1.2	1.8
	1.9	1.1	1.4	2.2	3.6	0.4	0.8	1.1	1.7
	2.0	1.1	1.3	2.0	3.4	0.4	0.7	1.1	1.6
	$EARL_{(0,2]}$ / $ESDRL_{(0,2]}$	10.2	13.0	19.4	31.1	6.4	8.5	13.2	22.1
	$\%\text{Diff}_{(0,2]}$		28.5%	90.7%	206.3%		33.0%	105.8%	245.0%

Table 2
The *ARL* and *SDRL* profiles of the HWMA $\bar{X}^*$ scheme (for the no remedy strategy) for different values of λ along with the corresponding design parameters when n=5, B=1, (ϕ,γ)=(0.5, 0.5) and ARL_0=500

		ARL				*SDRL*			
	(λ, L^*)	(0.05,2.609)	(0.1,2.938)	(0.25,3.074)	(0.5,3.089)	(0.05,2.609)	(0.1,2.938)	(0.25,3.074)	(0.5,3.089)
	0.0	500.4	504.0	504.1	498.2	373.8	407.2	486.9	492.8
	0.1	156.5	171.1	237.6	361.2	118.5	133.2	219.5	358.8
	0.2	60.7	67.8	91.3	184.6	43.6	46.0	78.7	179.1
	0.3	32.3	37.0	45.1	94.3	22.6	23.6	35.2	89.7
	0.4	20.3	23.4	26.8	52.5	13.7	14.3	19.3	48.3
	0.5	14.1	16.3	18.0	31.4	9.2	9.5	12.0	28.0
	0.6	10.3	12.0	12.8	20.3	6.4	6.9	8.0	17.7
	0.7	8.1	9.5	9.8	14.4	4.9	5.2	5.8	11.8
	0.8	6.6	7.6	7.8	10.5	3.8	4.1	4.4	8.2
δ	0.9	5.5	6.3	6.4	8.0	3.0	3.3	3.5	5.9
	1.0	4.8	5.4	5.4	6.3	2.6	2.7	2.8	4.4
	1.1	4.2	4.7	4.6	5.2	2.2	2.2	2.4	3.4
	1.2	3.7	4.1	4.0	4.3	1.9	1.9	2.0	2.7
	1.3	3.3	3.7	3.6	3.7	1.7	1.7	1.7	2.2
	1.4	3.0	3.4	3.2	3.2	1.5	1.5	1.5	1.8
	1.5	2.8	3.1	2.9	2.9	1.4	1.4	1.3	1.6
	1.6	2.5	2.8	2.7	2.6	1.3	1.3	1.2	1.4
	1.7	2.3	2.6	2.4	2.3	1.3	1.2	1.1	1.2
	1.8	2.1	2.4	2.2	2.1	1.2	1.2	1.0	1.0
	1.9	2.0	2.2	2.1	2.0	1.1	1.1	1.0	0.9
	2.0	1.8	2.0	1.9	1.8	1.0	1.1	0.9	0.8
	$EARL_{(0,2]}$ / $ESDRL_{(0,2]}$	17.33	19.35	24.52	40.69	12.14	13.17	20.16	38.44

Next, the effect of increasing s and m on the performance of the HWMA $\bar{X}^*$ scheme integrated with mixed-*s*&*m* sampling strategy is illustrated in Table 3. It is observed that as s and m increase, the *ARL*s, *SDRL*s, *EARL* and *ESDRL* decrease which indicates that the negative effect of autocorrelation and measurement errors is reduced. Thus, it follows that, whenever ϕ and γ are greater than 0, the HWMA $\bar{X}^*$ scheme integrated with mixed-*s*&*m* sampling strategy has a better performance than the HWMA $\bar{X}^*$ scheme with no remedy strategy. Note though, it is important to note that the use of the mixed-*s*&*m* sampling strategy requires more time and effort than the no remedy strategy. Consequently, a balance needs to be struck between performance and cost. Based on numerous simulations we conducted, we recommend a value of s equal to 1, 2, 3 and 4 for a ϕ within (0,0.3], (0.3,0.5], (0.5,0.7] and (0.7,1), respectively. Note though, for large datasets, the value of s can be increased further when $\phi \in$(0.7,1) because the level of autocorrelation has a much larger negative effect on the performance of the HWMA $\bar{X}^*$ scheme than the level of measurement errors. Next, we recommend a value of m equal to 1, 2 and 3 for a γ within (0,0.4], (0.4,0.8] and (0.8,1], respectively. Note that for $\gamma > 1$, a value of m = 4 can be used; however, $m > 4$ should never be used because the level of measurement errors do not have a significant negative effect on the performance of the HWMA $\bar{X}^*$ scheme as compared to the level of autocorrelation. Moreover, the cost and effort of R&R (repeatability & reproducibility)

associated with measurement errors is much higher as compared to skipping or mixing samples associated with autocorrelation.

Table 3
The ARL and $SDRL$ profiles of the HWMA $\bar{X}^*$ scheme (for the mixed-s&m strategy) with a constant variance when n=5, λ=0.1, ϕ=0.75, γ=0.75, L^*=2.938, ARL_0=500 with $s \in \{1,2,3,4\}$ and $m \in \{2,3,4,5\}$

		ARL					***SDRL***				
	(*s*,*m*)	**No remedy**	**(1,2)**	**(2,3)**	**(3,4)**	**(4,5)**	**No remedy**	**(1,2)**	**(2,3)**	**(3,4)**	**(4,5)**
	0.1	222.9	155.6	139.2	126.7	121.8	176.0	118.2	104.9	93.2	89.5
	0.2	93.9	59.9	52.7	47.5	44.8	66.9	39.7	35.2	31.6	29.0
	0.3	52.4	31.9	28.4	25.5	23.5	34.4	20.1	17.5	15.6	14.3
	0.4	33.4	20.4	17.8	16.0	15.0	21.0	12.3	10.5	9.5	8.6
	0.5	23.3	14.2	12.4	11.2	10.4	14.2	8.3	7.2	6.4	5.8
	0.6	17.7	10.5	9.2	8.3	7.7	10.5	6.0	5.0	4.5	4.2
	0.7	13.7	8.3	7.2	6.5	6.0	8.0	4.4	3.8	3.3	3.1
δ	0.8	11.0	6.6	5.9	5.4	4.9	6.2	3.4	3.0	2.7	2.4
	0.9	9.1	5.6	4.9	4.5	4.2	4.9	2.8	2.4	2.2	2.0
	1.0	7.6	4.7	4.2	3.9	3.7	4.0	2.3	2.0	1.8	1.7
	1.1	6.6	4.1	3.7	3.4	3.2	3.5	2.0	1.7	1.6	1.5
	1.2	5.7	3.7	3.3	3.0	2.8	2.9	1.7	1.5	1.4	1.3
	1.3	5.1	3.3	3.0	2.7	2.5	2.5	1.5	1.4	1.3	1.2
	1.4	4.6	3.0	2.7	2.5	2.3	2.2	1.4	1.3	1.2	1.1
	1.5	4.1	2.7	2.4	2.2	2.1	2.0	1.3	1.2	1.1	1.1
	1.6	3.8	2.5	2.2	2.0	1.9	1.7	1.2	1.1	1.1	1.0
	1.7	3.5	2.3	2.0	1.8	1.7	1.6	1.1	1.1	1.0	0.9
	1.8	3.2	2.1	1.9	1.7	1.5	1.5	1.1	1.0	0.9	0.8
	1.9	3.0	1.9	1.7	1.5	1.4	1.4	1.0	0.9	0.8	0.8
	2.0	2.8	1.8	1.6	1.4	1.3	1.3	1.0	0.9	0.8	0.7
	$EARL_{(0,2]}$ / $ESDRL_{(0,2]}$	26.4	17.3	15.3	13.9	13.1	18.3	11.5	10.2	9.1	8.5

Similarly, Fig. 2 shows that increasing the slope coefficient (i.e. B in Eq. (12b)) of the covariate error model yields an improvement in the performance of the HWMA $\bar{X}^*$ scheme with the mixed-s&m strategy (see Eq. (19a) and Eq. (19b)). That is, as B increases, the corresponding OOC ARL values decrease, for any constant input variables.

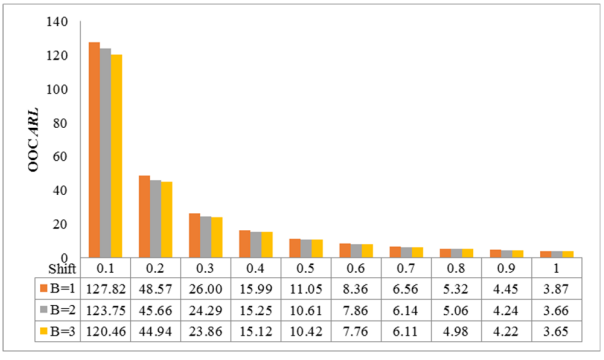

Fig. 2. The ARL profiles of the HWMA $\bar{X}^*$ scheme (for the mixed-3&4 strategy) with a constant variance when n=5, λ=0.1, ϕ=0.75, γ=0.75, L^*=2.938 and ARL_0=500 for different values of B

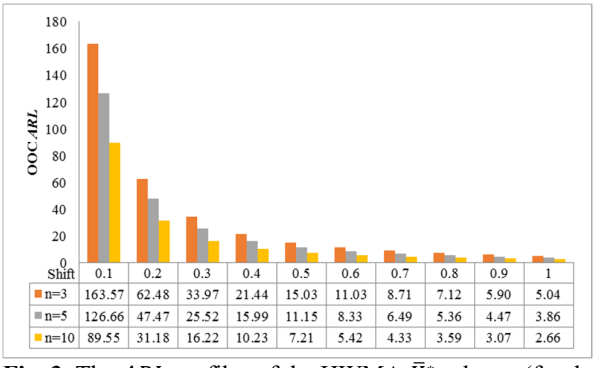

Fig. 3. The ARL profiles of the HWMA $\bar{X}^*$ scheme (for the mixed-3&4 strategy) with a constant variance when B=1, λ=0.1, ϕ=0.75, γ=0.75, L^*=2.938 and ARL_0=500 for different values of n

Finally, an increase in the sample size yields an improvement in the performance of the HWMA $\bar{X}^*$ scheme with the mixed-s&m strategy, see the illustration in Fig. 3 for $n \in \{3,5,10\}$. That is, the higher the sample size, the faster will the proposed monitoring scheme yields an OOC when there is actually shift in the process.

4.3 Sensitivity of the HWMA $\bar{X}^*$ scheme with linearly increasing variance

For the linearly increasing variance scenario, using Eq. (19a) and Eq. (19b) with the φ expression given in Eq. (12c), as C and D increase (with B fixed), the OOC ARL values increase indicating that the process deteriorates in performance. The latter is illustrated graphically for C and D in Fig. 4 and Fig. 5, respectively.

Although not shown here, for a fixed C and D, when the values of s and m are increased, the HWMA $\bar{X}^*$ scheme with the mixed-s&m strategy has an improved OOC performance (this is similar to the pattern in Table 2). Moreover, for a fixed C and D, when B is increased, the HWMA $\bar{X}^*$ scheme with the mixed-s&m strategy has an improved OOC performance (this is similar to the pattern in Fig. 2).

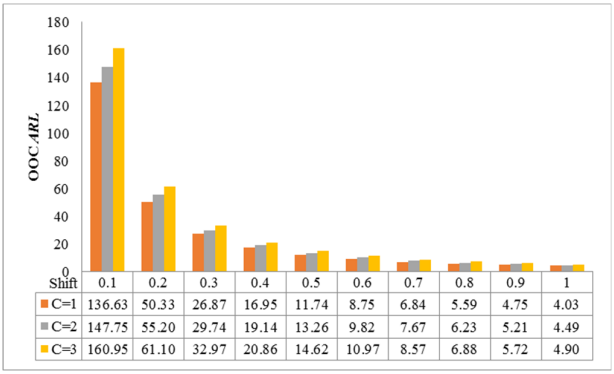

Shift	0.1	0.2	0.3	0.4	0.5	0.6	0.7	0.8	0.9	1
C=1	136.63	50.33	26.87	16.95	11.74	8.75	6.84	5.59	4.75	4.03
C=2	147.75	55.20	29.74	19.14	13.26	9.82	7.67	6.23	5.21	4.49
C=3	160.95	61.10	32.97	20.86	14.62	10.97	8.57	6.88	5.72	4.90

Fig. 4. The ARL profiles of the HWMA $\bar{X}^*$ scheme (for the mixed-3&4 strategy) with a linearly increasing variance when D=0, $C \in$\{1,2,3\} n=5, λ=0.1, ϕ=0.75, L^*=2.938 and ARL_0=500

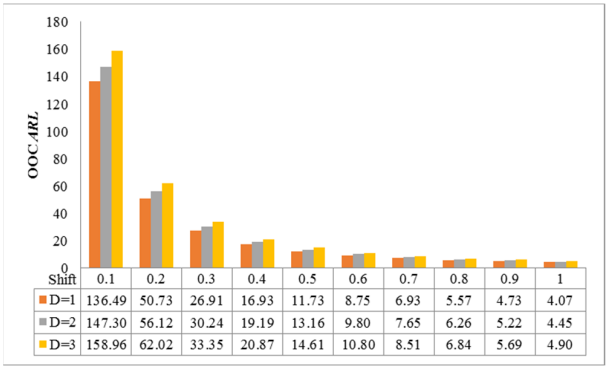

Shift	0.1	0.2	0.3	0.4	0.5	0.6	0.7	0.8	0.9	1
D=1	136.49	50.73	26.91	16.93	11.73	8.75	6.93	5.57	4.73	4.07
D=2	147.30	56.12	30.24	19.19	13.16	9.80	7.65	6.26	5.22	4.45
D=3	158.96	62.02	33.35	20.87	14.61	10.80	8.51	6.84	5.69	4.90

Fig. 5. The ARL profiles of the HWMA $\bar{X}^*$ scheme (for the mixed-3&4 strategy) with a linearly increasing variance when C=0, $D \in$\{1,2,3\}, n=5, λ=0.1, ϕ=0.75, L^*=2.938 and ARL_0=500

4.4 Comparison of different sampling strategies

For ease in plotting, let s and m be denoted by $(i-1)$ and i, respectively; then $i \in$\{1,2,…,10\} implies that $(s,m) \in$\{(0,1), (1, 2),…, (9,10)\}, with (0,1) sampling strategy denoting the 'no remedy' strategy. From (11a), it is observed that for the no remedy strategy, the autocorrelated process with constant measurement errors, its φ is given by

$$\varphi = \left(1 + 2\left(\frac{\phi^{n+1} - n\phi^2 + (n-1)\phi}{n(\phi-1)^2}\right)\right) + (B^2 + \gamma^2) - 1. \tag{24a}$$

However, that of the mixed-s&m strategy is given in (12b). Two additional methods used to reduce the negative effect of measurement errors and autocorrelation are s&m and mixed&m strategies, see Costa and Castagliola (2011) and Shongwe et al. (2021). The φ expressions for the two latter strategies are given by

$$\varphi = \left(1 + 2\left(\frac{\phi^{(s+1)(n+1)} - n\phi^{2s+2} + (n-1)\phi^{s+1}}{n(\phi^{s+1}-1)^2}\right)\right) + \left(B^2 + \frac{\gamma^2}{m}\right) - 1 \tag{24b}$$

and

$$\varphi = \left(\left(\frac{n_t}{n} + 2\left(\frac{\phi^{2n_t+2} - n_t\phi^4 + (n_t-1)\phi^2}{n(\phi^2-1)^2}\right)\right) + \left(\frac{n_{t-1}}{n} + 2\left(\frac{\phi^{2n_{t-1}+2} - n_{t-1}\phi^4 + (n_{t-1}-1)\phi^2}{n(\phi^2-1)^2}\right)\right)\right) + \left(B^2 + \frac{\gamma^2}{m}\right) - 1 \tag{24c}$$

When $0 < \phi, \gamma < 1$, then using (12b), (24a), (24b) and (24c), it is observed from Figure 6 that the φ values are greater than 1. For small values of ϕ and γ (e.g. ϕ=γ=0.25 in Figure 6(a)), the values of φ for the s&m and mixed-s&m strategies converge towards the value of 1; however, φ does not equal 1 exactly, which implies it is not theoretically possible to get rid of all the negative effect of autocorrelation and measurement errors.

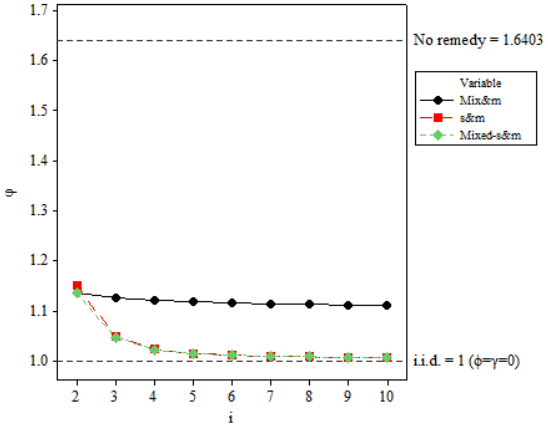

(a) ϕ=0.25 & γ=0.25

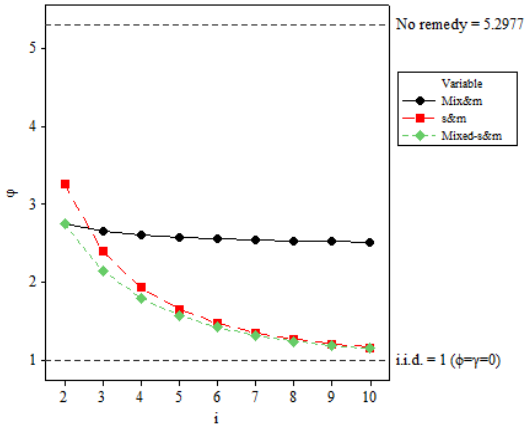

(b) ϕ=0.75 & γ=0.75

Fig. 6. The effect of different sampling strategies on φ when $(\phi, \gamma) \in$\{(0.25,0.25), (0.75,0.75)\}, n=10, $i \in$\{2,…,10\} or $(s,m) \in$\{(0,1), (1,2),…, (9,10)\}

For large values of ϕ and γ (e.g. ϕ=γ=0.75 in Fig. 6(b)), the values of φ for the s&m and mixed-s&m strategies only start getting close to a value of 1 at slightly higher values of s and m. The value of φ for the mix&m strategy is lower than the one

of the *s*&*m* strategy only when *s*=1 and *m*=2; otherwise, the converse is true. The no remedy strategy has a significantly large value of φ and should never be implemented as it yields the highest variability than any of the sampling strategies considered here; however, the mixed-*s*&*m* strategy yields a uniformly lower variability than all the considered strategies. Note that for the linearly increasing σ_M^2 scenario, a similar pattern (with slightly higher magnitudes) is observed for the values of φ. Next, in Table 4, the HWMA $\bar{X}^*$ scheme using the no remedy, mixed-&*m*, *s*&*m* and mixed-*s*&*m* strategies are compared against each other for an autocorrelated with constant and linearly increasing variance. It is observed that with respect to *ARL* and *EARL*, the sampling strategies can be sorted in the following order in terms of better OOC performance: mixed-*s*&*m* > *s*&*m* > mixed&*m* > 'no remedy'. That is, the run-length performance of the HWMA $\bar{X}^*$ scheme follows a similar pattern when using different sampling strategies as that shown in Fig. 6.

Table 4
The *ARL* profiles of the HWMA $\bar{X}^*$ scheme for different sampling strategies when n=5, λ=0.1, L^*=2.938, B=1, ARL_0=500 with *s*=3 and *m*=4

		ϕ=0.75, γ=0.75				ϕ=0.75, C=1, D=1			
	Strategy	No remedy	Mix&*m*	*s*&*m*	Mixed-*s*&*m*	No remedy	Mix&*m*	*s*&*m*	Mixed-*s*&*m*
	0.0	501.4	501.5	499.7	502.0	499.2	502.5	501.7	500.5
	0.1	223.0	149.9	143.1	129.3	259.9	163.3	158.3	149.5
	0.2	93.9	55.9	53.7	48.0	116.5	64.4	61.1	56.7
	0.3	52.1	30.4	28.7	25.6	66.1	34.7	33.4	30.0
	0.4	33.2	19.2	18.1	16.2	42.4	21.8	20.8	19.0
	0.5	23.3	13.4	12.4	11.1	30.2	15.4	14.6	13.2
	0.6	17.4	10.0	9.3	8.3	22.4	11.4	10.9	9.8
	0.7	13.5	7.7	7.3	6.5	17.6	8.9	8.4	7.7
δ	0.8	10.9	6.3	5.9	5.4	14.1	7.2	6.8	6.3
	0.9	9.1	5.3	5.0	4.5	11.7	6.0	5.7	5.2
	1.0	7.6	4.5	4.2	3.8	9.9	5.1	4.9	4.4
	1.1	6.6	3.9	3.7	3.4	8.5	4.4	4.3	3.9
	1.2	5.8	3.5	3.3	3.0	7.3	3.9	3.8	3.5
	1.3	5.1	3.1	3.0	2.7	6.5	3.5	3.3	3.1
	1.4	4.6	2.8	2.7	2.4	5.8	3.2	3.0	2.8
	1.5	4.1	2.6	2.4	2.2	5.2	2.9	2.8	2.6
	1.6	3.8	2.4	2.2	2.0	4.8	2.6	2.5	2.3
	1.7	3.5	2.1	2.1	1.9	4.4	2.4	2.3	2.1
	1.8	3.2	2.0	1.9	1.7	4.0	2.3	2.1	2.0
	1.9	3.0	1.8	1.7	1.5	3.7	2.1	2.0	1.8
	2.0	2.8	1.7	1.6	1.4	3.5	1.9	1.8	1.7
	$EARL_{(0,2]}$	26.32	16.42	15.62	14.04	32.22	18.37	17.64	16.37

Table 5
A comparison of the *ARL* and *EARL* profiles of the HWMA $\bar{X}^*$ scheme (and Shewhart $\bar{X}^*$ scheme in parentheses) with the mixed-*s*&*m* strategy when λ=0.1, k=3.0902 n=5, s=3, m=4, ARL_0=500 and $(\phi, \gamma) \in$ {(0.1,0.1),(0.3,0.3), (0.5,0.5), (0.7,0.7), (0.9,0.9)}

	(ϕ, γ)	(0.1,0.1)	(0.3,0.3)	(0.5,0.5)	(0.7,0.7)	(0.9,0.9)
	0	502.4 (500.0)	501.7 (500.0)	498.5 (500.0)	499.4 (500.0)	502.7 (500.0)
	0.1	95.4 (394.7)	97.6 (397.2)	106.1 (405.2)	129.6 (421.9)	196.2 (445.7)
	0.2	34.1 (232.3)	35.0 (236.3)	38.3 (249.8)	48.7 (280.7)	79.3 (332.0)
	0.3	18.2 (127.6)	18.1 (130.9)	20.1 (142.6)	25.8 (171.4)	43.0 (226.5)
	0.4	11.1 (71.2)	11.4 (73.6)	12.6 (82.0)	16.3 (103.9)	27.7 (150.5)
	0.5	7.8 (41.3)	8.1 (42.9)	8.8 (48.6)	11.4 (64.3)	19.6 (100.3)
	0.6	5.9 (25.0)	6.0 (26.0)	6.6 (29.9)	8.4 (40.9)	14.3 (67.8)
	0.7	4.7 (15.8)	4.8 (16.5)	5.2 (19.2)	6.6 (26.8)	11.1 (46.7)
δ	0.8	3.9 (10.4)	4.0 (10.9)	4.3 (12.7)	5.4 (18.1)	9.0 (32.8)
	0.9	3.3 (7.1)	3.4 (7.5)	3.7 (8.8)	4.6 (12.6)	7.5 (23.5)
	1.0	2.9 (5.1)	2.9 (5.4)	3.2 (6.3)	3.9 (9.0)	6.4 (17.2)
	1.1	2.5 (3.8)	2.6 (4.0)	2.8 (4.6)	3.5 (6.7)	5.5 (12.8)
	1.2	2.2 (2.9)	2.3 (3.1)	2.5 (3.5)	3.1 (5.1)	4.8 (9.7)
	1.3	2.0 (2.4)	2.0 (2.4)	2.2 (2.8)	2.7 (3.9)	4.3 (7.5)
	1.4	1.8 (1.9)	1.8 (2.0)	2.0 (2.3)	2.5 (3.2)	3.9 (5.9)
	1.5	1.6 (1.7)	1.6 (1.7)	1.8 (1.9)	2.3 (2.6)	3.5 (4.8)
	1.6	1.4 (1.5)	1.5 (1.5)	1.6 (1.7)	2.0 (2.2)	3.2 (3.9)
	1.7	1.3 (1.3)	1.3 (1.4)	1.5 (1.5)	1.9 (1.9)	3.0 (3.3)
	1.8	1.2 (1.2)	1.2 (1.2)	1.4 (1.3)	1.7 (1.7)	2.8 (2.8)
	1.9	1.1 (1.1)	1.2 (1.2)	1.3 (1.2)	1.6 (1.5)	2.6 (2.4)
	2.0	1.1 (1.1)	1.1 (1.1)	1.2 (1.2)	1.4 (1.4)	2.4 (2.1)
	$EARL_{(0,1]}$	18.72 (93.05)	19.13 (94.71)	20.89 (100.49)	26.06 (114.97)	41.39 (144.30)
	$PCI_{(0,1]}$	4.97	4.95	4.81	4.41	3.49
	$EARL_{(1,2]}$	1.62 (1.89)	1.65 (1.95)	1.81 (2.20)	2.26 (2.99)	3.59 (5.52)
	$PCI_{(1,2]}$	1.16	1.18	1.22	1.32	1.54
	$EARL_{(0,2]}$	10.17 (47.47)	10.39 (48.33)	11.35 (51.35)	14.16 (58.98)	22.49 (74.91)
	$PCI_{(0,2]}$	4.67	4.65	4.53	4.17	3.33

4.5 Comparison with the existing k-sigma limits Shewhart $\bar{X}^*$ scheme

The *ARL* and *EARL* profiles of the HWMA and Shewhart $\bar{X}^*$ schemes when $(\phi,\gamma) \in \{(0,0),(0.2,0.2), (0.5,0.5), (0.9,0.9)\}$ specifically for s=3 and m=4 are compared to each other in Table 5. For comparison purpose, the performance comparison index (*PCI*) is used to measure the relative effectiveness of two different schemes, which is given by

$$PCI_{(\delta_{\min},\delta_{\max}]} = EARL^{\text{Shewhart}}_{(\delta_{\min},\delta_{\max}]}/EARL^{\text{HWMA}}_{(\delta_{\min},\delta_{\max}]},$$

where $EARL^{\text{Shewhart}}_{(\delta_{\min},\delta_{\max}]}$ ($EARL^{\text{HWMA}}_{(\delta_{\min},\delta_{\max}]}$) is the *EARL* of Shewhart $\bar{X}^{\#}$ (HWMA $\bar{X}^{\#}$) scheme over the range of shifts from $\delta_{\min}$ to $\delta_{\max}$, respectively. When the *PCI* is equal to 1, greater than 1 or less than 1, it implies that the HWMA $\bar{X}^{\#}$ scheme has the same, better or worse performance than the Shewhart $\bar{X}^{\#}$ scheme, respectively. For the majority of the shifts in Table 5, it is apparent that the HWMA $\bar{X}^*$ scheme has a significantly better OOC *ARL* performance than the Shewhart $\bar{X}^*$ scheme. In addition, for different values of ϕ and γ, when $\delta \in$ (0,1], (1,2] and (0,2], the *ARL* and *EARL* of the HWMA $\bar{X}^*$ scheme outperforms those of the Shewhart $\bar{X}^*$ scheme since all the *PCI*s for different ranges of shifts are greater than 1. A similar pattern is observed when comparing the corresponding *SDRL*s and *ESDRL*s. Although not shown here, a similar pattern is also observed for other different values of *s* and *m*, as well as when the autocorrelated processes are subjected to linearly increasing σ_M^2. Hence, the HWMA $\bar{X}^*$ scheme has a better OOC performance and should be implemented instead of the existing Shewhart $\bar{X}^*$ scheme.

5. Illustrative example

In this section, the yogurt cup filling process dataset taken from Costa and Castagliola (2011) which shows the weights of different yogurt cups taken at different sampling points, is used to demonstrate the application and implementation of the HWMA $\bar{X}^*$ under the combined effect of measurement and autocorrelation using the mixed-*s*&*m* strategy. The dataset contains 20 samples each of size 5 taken every hour and each of them weighted two times (i.e. *m*=2). Historical information of this process indicated that the weight of a yogurt cup, denoted as $X^*_{t,i,j}$, fits an AR(1) model with parameter ϕ=0.38, an IC mean, μ_0=124.9g and an IC standard deviation, σ_0=0.76g. An R&R study indicates that the measurement system standard deviation, σ_M=0.24g, so that γ=0.316. The aim of this example is to show how to implement the mixed-*s*&*m* sampling strategy to form rational subgroups of size *n*=3 (i.e., with n_{t-1}=1 and n_t=2) when $s \in$ {1,2}, m=2. The plotting statistics at each sampling point for the mixed-1&2 and mixed-2&2 sampling strategies are shown in Table 6. For instance, for s=m=2 and t=3, the plotting statistic is calculated as follows:

$$\bar{X}^*_3 = \frac{1}{3}\left(\frac{X_{2,1,1}+X_{2,2,1}}{2}\right) + \frac{2}{3}\left(\frac{X_{3,1,1}+X_{3,1,4}+X_{3,2,1}+X_{3,2,4}}{4}\right) = \frac{1}{3}\left(\frac{124.9+125.2}{2}\right) + \frac{2}{3}\left(\frac{125.1+122.9+125.1+122.4}{4}\right) = 124.27,$$

with $\bar{\bar{X}}^*_2 = 125.03$, so that

$$H^*_3 = \lambda\bar{X}^*_3 + (1-\lambda)\,\bar{\bar{X}}^*_2 = 0.1(124.27) + (1-0.1)125.03 = 124.96.$$

In this example, when s=m=2, φ is found to be equal to 1.0322 so that the lower and upper control limits of the HWMA $\bar{X}^*$ scheme when $t = 3$ are calculated using Eq. (19a) and Eq. (19b) as follows:

$$LCL_3 = 124.90 - 2.938\sqrt{\left(\frac{0.1^2 \times (0.76)^2}{3} + \frac{(1-0.1)^2 \times (0.76)^2}{3\times(2-1)}\right)(1.0322)} = 124.06, \quad (25a)$$

and

$$UCL_3 = 124.90 + 2.938\sqrt{\left(\frac{0.1^2 \times (0.76)^2}{3} + \frac{(1-0.1)^2 \times (0.76)^2}{3\times(2-1)}\right)(1.0322)} = 125.74. \quad (25b)$$

Other time-varying control limits for $t > 1$ can also be calculated in a similar way as shown in (25a) and (25b), respectively. The plotting statistics and control limits of the HWMA $\bar{X}^*$ scheme when (*s*,*m*) = (1,2) and (2,2) are displayed in Table 6 and Fig. 7. For this specific example, the signal is observed for the first time on the 15th subgroup in both cases.

Table 6

Illustration of the charting statistics of the HWMA $\bar{X}^*$ scheme using the yogurt cup filling data when n=3 (i.e., with n_{t-1}=1 and n_t=2) when $s \in \{1,2\}$ and m=2

	First set					Second set																	
														s=1,*m*=2						*s*=2,*m*=2			
t	$X^*_{t,1,1}$	$X^*_{t,2,1}$	$X^*_{t,3,1}$	$X^*_{t,4,1}$	$X^*_{t,5,1}$	$X^*_{t,1,2}$	$X^*_{t,2,2}$	$X^*_{t,3,2}$	$X^*_{t,4,2}$	$X^*_{t,5,2}$	$\bar{X}^*_t$	$\bar{\bar{X}}^*_{t-1}$	H^*_t	LCL_t	UCL_t	Signal	$\bar{X}^*_t$	$\bar{\bar{X}}^*_{t-1}$	H^*_t	LCL_t	UCL_t	Signal
1	124.90	125.90	125.20	124.60	124.80	124.80	125.90	124.80	124.10	124.40				124.77	125.03	No				124.77	125.03	N
2	124.90	125.50	124.10	125.20	125.00	125.20	125.00	123.90	125.20	125.60	124.63	124.90	124.87	123.70	126.10	No	125.03	124.90	124.91	123.71	126.09	N
3	125.10	125.20	125.40	122.90	125.40	125.10	124.80	125.30	122.40	125.40	125.17	124.63	124.69	124.04	125.76	No	124.27	125.03	124.96	124.06	125.74	N
4	126.10	124.60	125.70	126.40	124.90	125.90	124.80	125.50	126.50	125.70	125.57	124.90	124.97	124.20	125.60	No	125.85	124.65	124.77	124.21	125.59	N
5	125.80	122.60	124.10	126.10	124.90	125.70	122.60	123.50	126.30	125.00	125.18	125.12	125.13	124.29	125.51	No	125.98	125.05	125.14	124.30	125.50	N
6	125.00	125.50	124.80	124.90	124.80	125.20	124.80	125.00	124.80	124.20	125.25	125.14	125.15	124.35	125.45	No	125.23	125.28	125.28	124.36	125.44	N
7	124.20	125.80	125.40	126.40	125.10	124.60	125.30	125.50	126.20	125.20	124.98	125.16	125.14	124.39	125.41	No	125.27	125.27	125.27	124.40	125.40	N
8	124.90	123.80	125.10	124.00	124.40	124.90	123.20	125.30	124.50	124.20	124.83	125.13	125.10	124.43	125.37	No	124.52	125.27	125.20	124.44	125.36	N
9	125.90	124.40	126.30	124.90	125.20	125.80	124.80	125.70	125.20	125.10	125.58	125.09	125.14	124.46	125.34	No	125.27	125.16	125.17	124.46	125.34	N
10	124.20	126.20	125.60	124.40	124.10	124.30	125.50	125.00	124.40	124.30	125.13	125.15	125.15	124.48	125.32	No	124.83	125.18	125.14	124.49	125.31	N
11	123.70	123.40	124.70	123.10	123.10	123.60	123.30	124.80	123.10	122.80	124.22	125.15	125.06	124.50	125.30	No	123.67	125.14	124.99	124.50	125.30	N
12	124.00	122.60	123.60	124.40	123.60	124.10	122.40	123.60	124.50	123.10	123.77	125.06	124.93	124.52	125.28	No	124.05	124.99	124.90	124.52	125.28	N
13	122.00	123.90	123.70	124.30	121.90	122.50	124.00	124.10	124.40	122.90	123.40	124.94	124.78	124.53	125.27	No	123.55	124.91	124.77	124.54	125.26	N
14	122.40	122.80	123.70	123.70	122.80	123.00	123.10	124.20	124.10	123.10	122.97	124.81	124.63	124.54	125.26	No	122.95	124.79	124.61	124.55	125.25	N
15	123.90	124.10	123.40	123.10	124.50	123.60	124.50	122.90	123.10	125.10	123.20	124.67	124.52	124.55	125.25	Yes	123.18	124.65	124.50	124.56	125.24	Ye
16	121.90	123.40	123.50	125.30	123.30	122.30	123.30	123.30	125.50	123.60	123.08	124.56	124.42	124.56	125.24	Yes	123.75	124.55	124.47	124.57	125.23	Ye
17	123.30	123.60	124.20	123.40	123.50	122.90	123.50	123.80	123.60	123.40	123.07	124.46	124.32	124.57	125.23	Yes	122.90	124.49	124.33	124.58	125.22	Ye
18	122.00	123.60	124.70	122.60	124.50	122.20	123.40	125.00	122.50	123.90	123.35	124.38	124.27	124.58	125.22	Yes	122.58	124.39	124.21	124.59	125.21	Ye
19	124.00	123.10	123.90	122.60	124.20	123.90	123.40	124.50	122.80	123.50	123.42	124.32	124.23	124.59	125.21	Yes	122.92	124.29	124.15	124.59	125.21	Ye
20	125.50	122.20	123.20	123.20	123.20	124.90	122.30	123.20	123.30	123.20	124.12	124.27	124.25	124.60	125.20	Yes	124.13	124.21	124.20	124.60	125.20	Ye

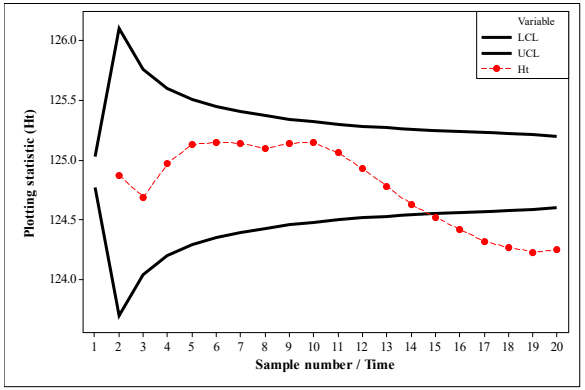

(a) $(s,m) = (1,2)$

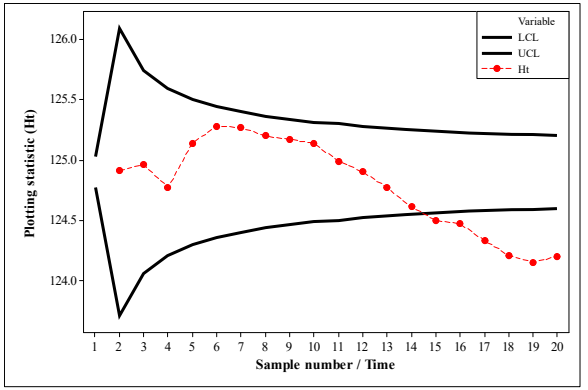

(b)

Fig. 7. HWMA $\bar{X}^*$ scheme using the mixed-*s*&*m* strategy for the yogurt cup filling data when n=3 (i.e., with n_{t-1}=1 and n_t=2) when $s \in \{1,2\}$ and m=2

6. Concluding remarks

A new HWMA scheme to monitor the process means under the effect of within-sample correlation with and without measurement errors are proposed. To reduce the negative effect of autocorrelation and measurement errors, sampling strategies that involve skipping and mixing different samples are integrated into the HWMA scheme's design. Then, using Monte Carlo simulations, it is shown that the HWMA scheme using the mixed-*s&m* strategy has a uniformly better OOC performance than its competitors when the process is under the combined effect of autocorrelation and measurement errors (for both constant and linearly increasing variance). A comparison with the only existing basic Shewhart scheme using the mixed-*s&m* strategy indicates that the new HWMA scheme is more efficient in quick detection of shifts. Although the results in this study were illustrated for a few different sample sizes, the same conclusion holds for other values of n (or, n_t and n_{t-1}). For future research, this study will be conducted by taking into account parameter estimation effect. Also, the use of the mixed-*s&m* strategies needs to be thoroughly studied for other memory-type monitoring schemes (i.e. CUSUM, EWMA and GWMA).

References

Abbas, N. (2020). Homogeneously weighted moving average control chart with an application in substrate manufacturing process. *Computers & Industrial Engineering*, *120*, 460-470.

Abbas, N., Riaz, M., Ahmad, S., Abid, M., & Zaman, B. (2020). On the efficient monitoring of multivariate processes with unknown parameters. *Mathematics*, *8*(5), 823.

Abid, M., Shabbir, A., Nazir, H.Z., Sherwani, R.A.K., & Riaz, M. (2020a). A double homogeneously weighted moving average control chart for monitoring of the process mean. *Quality and Reliability Engineering International*, *36*(5), 1513-1527.

Abid, M., Mei, S., Nazir, H.Z., Riaz, M., & Hussain, S. (2020b). A mixed HWMA-CUSUM mean chart with an application to manufacturing process. *Quality and Reliability Engineering International*, *37*(2), 618-631.

Adegoke, N.A., Smith, A.N.H., Anderson, M.J., Sanusi, R.A., & Pawley, M.D.M. (2019a). Efficient homogeneously weighted moving average chart for monitoring process mean using an auxiliary variable. *IEEE Access*, *7*, 94021-94032.

Adegoke, N.A., Abbasi, S.A., Smith, A.N.H., Anderson, M.J., & Pawley, M.D.M. (2019b). A multivariate homogeneously weighted moving average control chart. *IEEE Access*, *7*, 9586-9597.

Adeoti, O.A., & Koleoso, S.O. (2020). A hybrid homogeneously weighted moving average control chart for process monitoring. *Quality and Reliability Engineering International*, *36*(6), 2170-2186.

Ahmad, S., Riaz, M., Hussain, S., & Abbasi, S.A. (2019). On auxiliary information-based control charts for autocorrelated processes with application in manufacturing industry. *The International Journal of Advanced Manufacturing Technology*, *100*(5-8), 1965-1980.

Alevizakos, V., Chatterjee, K., & Koukouvinos, C. (2021). The extended homogenously weighted moving average control chart. *Quality and Reliability Engineering International*, DOI: 10.1002/qre.2849

Alwan, L.C., & Radson, D. (1992). Time-series investigation of subsample mean chart. *IIE Transactions*, *24*(5), 66-80.

Arif, F., Noor-ul-Amin, M., & Hanif, M. (2020). Joint monitoring of mean and variance using likelihood ratio test statistic with measurement error. *Quality Technology & Quantitative Management, 18*(2), 202-224.

Asif, F., Khan, S., & Noor-ul-Amin, M. (2020). Hybrid exponentially weighted moving average control chart with measurement error. *Iranian Journal of Science and Technology, Transactions A: Science*, *44*(3), 801-811.

Aslam, M., Saghir, A., & Ahmad, L. (2020). *Introduction to Statistical Process Control*, Hoboken, NJ, USA: Wiley.

Costa, A.F.B., & Castagliola, P. (2011). Effect of measurement error and autocorrelation on the $\bar{X}$ chart. *Journal of Applied Statistics, 38*(4), 661-673.

Dargopatil, P., & Ghute, V. (2019). New sampling strategies to reduce the effect of autocorrelation on the synthetic T^2 chart to monitor bivariate process. *Quality and Reliability Engineering International*, *35*(1), 30-46.

Dawod, A., Adegoke, N.A., & Abbasi, S.A. (2020). Efficient linear profile schemes for monitoring bivariate correlated processes with applications in the pharmaceutical industry. *Chemometrics and Laboratory Systems*, *206*, 104137.

Franco, B.C., Castagliola, P., Celano, G., & Costa, A.F.B. (2014). A new sampling strategy to reduce the effect of autocorrelation on a control chart. *Journal of Applied Statistics*, *41*(7), 1408-1421.

Linna, K.W., & Woodall, W.H. (2001). Effect of measurement error on Shewhart control charts. *Journal of Quality Technology*, *33*(2), 213-222.

Maleki, M.R., Amiri, A., & Castagliola, P. (2017). Measurement errors in statistical process monitoring: A literature review. *Computers & Industrial Engineering*, *103*, 316-329.

Malela-Majika, J.-C., Shongwe, S.C., & Adeoti, O.A. (2021). A hybrid homogenously weighted moving average control chart for process monitoring: Discussion. *Quality and Reliability Engineering International*, DOI: 10.1002/qre.2911.

Maravelakis, P., Panaretos, J., & Psarakis, S. (2004). EWMA chart and measurement error. *Journal of Applied Statistics, 31*(4), 445-455.

Maravelakis, P. (2012). Measurement error on the CUSUM control chart. *Journal of Applied Statistics*, *39*(2), 323-336.

Montgomery, D.C. (2013). *Statistical Quality Control: A Modern Introduction*, 7th ed., Singapore: John Wiley & Sons.

Nawaz, T., & Han, D. (2020). Monitoring the process location by using new ranked set sampling based memory control charts. *Quality Technology & Quantitative Management*, *17*(3), 255-284.

Nguyen, H.D., Nguyen, Q.T., Nguyen, T.H., Balakrishnan, N., & Tran, K.P. (2020). The performance of the EWMA median chart in the presence of measurement error. *Artificial Intelligence Evolution*, *1*(1), 48-62.

Oh, J., & Weiβ, C.H. (2020). On the individuals chart with supplementary runs rules under serial dependence. *Methodology and Computing in Applied Probability*, *22*, 1257-1273.

Prajapati, D.R., & Singh, S. (2012). Control charts for monitoring the autocorrelated process parameters: A literature review. *International Journal of Productivity and Quality Management*, *10*(2), 207-249.

Raza, M., Nawaz, T., & Han, D. (2020). On designing distribution-free homogeneously weighted moving average control charts. *Journal Testing and Evaluation, 48*(4), 3154-3171.

Shongwe, S.C., Malela-Majika, J.-C., & Castagliola, P. (2020). The new synthetic and runs-rules schemes to monitor the process mean of autocorrelated observations with measurement errors. *Communications in Statistics – Theory and Methods*, DOI: 10.1080/03610926.2020.1737125.

Shongwe, S.C., & Malela-Majika, J.-C. (2020). A new variable sampling size and interval synthetic and runs-rules schemes to monitor the process mean of autocorrelated observations with measurement errors. *International Journal of Industrial Engineering Computations*, *11*(4), 607-626.

Shongwe, S.C., Malela-Majika, J.-C., & Castagliola, P. (2021). A combined mixed-*s*-skip sampling strategy to reduce the effect of autocorrelation on the $\bar{X}$ scheme with and without measurement errors. *Journal of Applied Statistics*, *48*(7), 1243-1268.

Thanwane, M., Malela-Majika, J.-C., Castagliola, P., & Shongwe, S.C. (2020). The effect of measurement errors on the performance of the homogeneously weighted moving average $\bar{X}$ monitoring scheme. *Transactions of the Institute of Measurement and Control, 43*(3), 728-745.

Xiaohong, L., & Zhaojun, W. (2009). The CUSUM control chart for the autocorrelated data with measurement error. *Chinese Journal of Applied Probability*, *25*(5), 461-474.

Yang, S.F., & Yang, C.M. (2005). Effects of imprecise measurement on the two dependent processes control for the autocorrelated observations. *The International Journal of Advanced Manufacturing Technology, 26*(5-6), 623-630.

Zaidi, F., Castagliola, P., Tran, K.P., & Khoo, M.B.C. (2020). Performance of the MEWMA-CoDa control chart in the presence of measurement errors. *Quality and Reliability Engineering International*, *36*(7), 2411-2440.